The Failure of "Classic" Perturbation Theory at a Rough Neumann Boundary Near Grazing

Donald E. Barrick and Rosa Fitzgerald

Abstract—Rice's "classic" perturbation theory predicts an erroneous limit at grazing for vertically polarized plane wave scatter from an infinite perfectly conducting rough surface; likewise, the attendant result for the specularly reflected mode also fails at grazing. We show where and why in the system of perturbational equations this difficulty occurs. We then reformulate the perturbational approach to handle the low-incidence angle region for a one-dimensionally (1-D) rough Neumann boundary (vertical polarization from a perfectly conducting surface). The result for scattered fields vanishes in direct proportion to incidence angle above grazing and the result for the normalized roughness-modified surface impedance becomes constant with angle near grazing. For completeness and comparison, we give results for the horizontal polarization at a Dirichlet boundary, where perturbation results encounter no difficulties. Scatter dependence on grazing angle is explained in terms of the "classic" perturbation result multiplied by a propagation factor to the cell. The latter includes the sum of the direct and specularly reflected waves at the surface. This quantity can be replaced by the appropriate surface-wave propagation factor for radiation from dipole antennas, thereby explaining the strong observed vertically polarized sea scatter at high frequency (HF) on and below the horizon.

Index Terms—Electromagnetic (EM) scattering from rough surfaces, perturbation methods.

I. INTRODUCTION

DR. James R. Wait led the way in the west in applying surface impedance concepts to both propagation and scatter of vertically polarized waves at planar and spherical boundaries. His classic text *Electromagnetic Waves in Stratified Media* [1] is based entirely on this description of earth and sea interfaces. Wait also showed [2] how roughness on a curved conducting boundary modifies its near-grazing impedance, which prior to that had been derived by Barrick [3] and Feynberg [4] only for planar boundaries. Unravelling the perturbation theory failure conundrum—the purpose of this manuscript—is all based on the connections between roughness, the surface impedance/admittance, and scatter on which Dr. Wait has shed pioneering light.

Propagation and scatter of vertically polarized electromagnetic (EM) waves near grazing above a slightly rough perfectly conducting surface is fraught with a number of inconsistencies. For two-dimensional (2-D) fields above a one-dimensional

(1-D) profile for this polarization, the conducting surface becomes the Neumann or "hard" boundary condition; for easier understanding, we restrict study to the 1-D geometry. Lord Rayleigh [5] used perturbation theory to derive scattered fields from a sinusoidal Neumann boundary more than a century ago; Rice [6] was the first to apply the same technique to arbitrary periodic and randomly rough surfaces.

A. Scatter Theory

Rice's perturbation theory [6] leads to the following result for the normalized in-plane bistatic scatter cross section from a statistically rough 1-D Neumann boundary with roughness height spectrum $S(\kappa)$ at the surface wavenumber κ that satisfies the Bragg condition $\kappa = k(\cos\alpha - \cos\beta)$

$$\sigma_{vv}^{o} = \pi k^3 S(k(\cos\alpha - \cos\beta))(1 - \cos\alpha\cos\beta)^2$$

where

k radio wavenumber;
α incidence angle above grazing;
β scatter angle above grazing with respect to the forward direction.

Thus, for backscatter, $\beta = \pi - \alpha$ and $\cos\beta = -\cos\alpha$. We refer to this equation and its three-dimensional (3-D) counterparts (e.g., Tatarskii and Charnotskii [7], [8]) "as "classic" perturbation results in our subsequent discussions. Power does not vanish as it should above any dissipative surface when grazing is approached.

B. Propagation and Energy Conservation

The above inconsistency of the "classic" perturbation solution for scatter is attended by contradictions in the fields propagating across the surface as grazing is approached. For incident plane wave excitation, we define the propagating field as the "space wave," which includes the incident and the specularly reflected plane waves. The latter is often referred to as the "coherent" component of scatter from statistically rough surfaces. In the grazing limit, the two components of the space wave merge into a single forward propagating field.

Rice [6] gives expressions from perturbation theory through second order for the first two terms of the specularly reflected plane wave from a perfectly conducting slightly rough surface. This is expressed as as a Fresnel-like coherent reflection coefficient. We repeat [6, eq. (5.5)] based on [6, eqs. (4.3) and (3.25)]

$$R_V = +1 - \frac{s_h}{\gamma}; \quad R_H = -1 + \gamma s_p$$

where the first equation applies to vertical polarization (the Neumann 1-D boundary) and the second to horizontal (the Dirichlet 1-D boundary). In Rice's words, " ...γ is the cosine of the angle between the vertical and the reflected ray," and " ..., s_p, s_h stand for small quantities." Thus, $\gamma = \sin\alpha$ using our definition.

For horizontal polarization (Dirichlet boundary), the second equation behaves like a plane wave Fresnel reflection at any planar interface between free-space and a lower, denser, and homogeneous medium; it approaches -1 in the grazing limit. The above equation for vertical polarization (Neumann boundary) has a big problem at grazing: the second term dominates and the reflected field goes to infinity. Hence, energy conservation is grossly violated, as the power in the incident (causative) plane wave was taken to be constant. This breakdown for reflection should sound an alarm that the preceding scatter results near grazing must be suspect also, both having been derived from the same system of equations.

In the next section, we revisit "classic" perturbation theory for a Neumann boundary, using our more exact modal formulation [9], [10], which avoids the Rayleigh hypothesis. We show exactly how and where the perturbational system of equations fail at grazing. In Section III, we derive perturbation solutions for scatter and propagation that are valid and exact in the grazing limit. In Section IV, we reconcile the two seemingly different perturbational approaches, examining the transition zone between the two; we also clarify the inextricable interconnection between scatter and propagation in this important limit and resolve the quandary of why high-frequency (HF) radars at grazing see such a strong sea scatter echo. Section V considers horizontal polarization for a Dirichlet boundary, deriving an admittance counterpart to the Neumann impedance and examining propagation and scatter behavior near grazing.

II. WHY "CLASSIC" PERTURBATION FAILS AT GRAZING

A. Review of Modal Formulation

Barrick [9], [10] presents an exact formulation for 2-D propagation and scatter above any arbitrary 1-D rough periodic Neumann boundary with height $\zeta(x)$ and fundamental period L. Unlike earlier approaches of Rice [6], Wait [2], and Barrick [3], [11] that invoke the Rayleigh hypothesis, [10] avoids this assumption that the fields are approximated by only upgoing modes in the region between crests and troughs. Rather, solution follows a two-step process where unknown surface-current Fourier coefficients are first determined from a simple system of equations with only one nonzero element on the right; these coefficients are then multiplied by a known matrix to find the reflected and scattered field modal amplitudes. Thus, we have [9], [10]

$$[P_{mn}][S_n] = [2\sin\alpha\,\delta_m^0] \quad \text{and} \quad [Q_{mn}][S_n] = [2\chi_m H_m].$$
$$(1)$$

Here, S_n and H_m are the unknown surface-current Fourier coefficients and the scattered-field modal amplitudes, respectively,

defined with respect to the y-directed magnetic field $h_y(x,z)$ by

$$
h_y^s(x,\zeta(x))
$$
$$
= \sum_{n=-\infty}^{+\infty} S_n e^{in\kappa x - ik\cos\alpha x} \quad \text{(on the surface)} \qquad (2a)
$$
$$
h_y^s(x,z)
$$
$$
= \sum_{m=-\infty}^{+\infty} H_m e^{im\kappa x - ik\cos\alpha x + i\kappa_m z} \quad \text{for } z > \zeta_{\text{Max}}
$$
$$(2b)$$

where

$$
\kappa_m \equiv k\chi_m, \quad \chi_m \equiv \sqrt{1-\xi_m^2}, \quad \text{and}
$$
$$
\xi_m \equiv \cos\alpha - \frac{m\kappa}{k} \qquad (3)
$$

where

k radio wavenumber;
$\kappa = 2\pi/L$ fundamental wavenumber for the periodic surface;
α angle from grazing of the incident plane wave

$$
h_y^i = e^{-ik\cos\alpha x - ik\sin\alpha z - i\omega t} \qquad (4)
$$

and, henceforth, the time-dependent exponential factor is omitted but implied.

The matrices $[P_{mn}]$ and $[Q_{mn}]$ are defined from Green's integral equations [10, eqs. (4), (5)], e.g., for the Neumann boundary the relevant equation giving P_{mn} becomes

$$
\int_0^L \left[\kappa_m - \xi_m \frac{\partial\zeta(x)}{\partial x}\right] \exp[i\xi_m x + i\kappa_m \zeta(x)]
$$
$$
\times h_y^s(x,\zeta(x))\,dx = 2kL\sin\alpha\,\delta_m^0 \qquad (5)
$$

where δ_m^0 in (1) and (5) is the Kronecker delta, implying that only one term on the right side of (1a) involving S_n is nonzero. For the Neumann boundary the matrix coefficients required on the left sides of (1) become

$$
P_{mn} = \left[\frac{1-\xi_m\xi_n}{\chi_m}\right] \cdot p_{n-m}^m \quad \text{and}
$$
$$
Q_{mn} = \left[\frac{1-\xi_m\xi_n}{\chi_m}\right] \cdot q_{n-m}^m. \qquad (6)
$$

B. Applying Perturbation

The surface profile height enters through the coefficients p_j^m and q_j^m. These are defined [9], [10] as the Fourier coefficients of the height characteristic functions $\exp[\pm i\kappa_m \zeta(x)]$. In the perturbation limit of small heights, the exponential is expanded in its first terms resulting in the following reductions for these quantities:

$$
\left.\begin{matrix} p_{n-m}^m \\ q_{n-m}^m \end{matrix}\right\} = 1 \pm ik\chi_m z_{n-m} - (k\chi_m)^2 v_{n-m} + \qquad (7a)
$$

with the coefficients of the surface height and its square defined from

$$\zeta(x) = \sum_{m=-\infty}^{+\infty} z_m e^{im\kappa x} \quad \text{and} \quad \zeta^2(x) = \sum_{m=-\infty}^{+\infty} v_m e^{im\kappa x}. \tag{7b}$$

With the above equations defining the scatter process in the small surface-height limit, one employs the methodology in [9, appendix] to set up the "classic" perturbation equations [9, eq. (A1), (A2)]. For clarity we show the process applied to a sinusoidal profile at grazing in which only two surface coefficients z_1 and z_{-1} are nonzero. This is extended by inspection to the general case of more complex surfaces involving $z_{\pm n}$ up through $|n| = N$. Hence, we need show only three equations of the set represented by (1) above since only these three have terms larger than "order three" (denoted $O(3)$) in the perturbation parameter kz_n. The upper/lower line and signs represent the first and second of (1), respectively,

$$\pm ikz_1(1 - \xi_{-1}\xi_{-2})S_{-2} + \chi_{-1}S_{-1} \pm ikz_{-1}$$
$$\times (1 - \xi_{-1}\cos\alpha)S_0 + O(3) = \begin{cases} 0 \\ 2\chi_{-1}H_{-1} \end{cases} \tag{8a}$$
$$\pm ikz_1(1 - \xi_{-1}\cos\alpha)S_{-1} + \lceil 1 - (k\sin\alpha)^2 v_0 \rceil S_0 \sin\alpha \pm ikz_{-1}$$
$$\times (1 - \xi_1\cos\alpha)S_1 + O(3) = \begin{cases} 2\sin\alpha \\ 2\sin\alpha H_0 \end{cases} \tag{8b}$$
$$\pm ikz_1(1 - \xi_1\cos\alpha)S_0 + \chi_1 S_1 \pm ikz_{-1}$$
$$\times (1 - \xi_1\xi_2)S_2 + O(3) = \begin{cases} 0 \\ 2\chi_1 H_1 \end{cases}. \tag{8c}$$

C. Scatter Solutions

In the "classic" perturbation approach, it is assumed that the grazing angle α and, thus $\sin\alpha$, in the above equations is an independent variable and, hence, not necessarily small. In this case, the first and third terms on the left of (8b) are at least first order (we shall see these are actually second order in kz_n) and only the middle term involving S_0 remains to lowest order. Hence, solving the upper set of (8b), this zero-order term is equated to the right side (with the common $\sin\alpha$ factor canceling) to give $S_0^{(0)} = 2$, where superscript denotes the smallness order in the perturbation parameter. When this is substituted into (8a), the rightmost term with S_0 is first order; the middle term in S_{-1} must, hence, be at least first order and, thus, S_n in general for $n \neq 0$ must be at least first order. This leads to solutions to first order in kz_n for the surface-current coefficients

$$S_n^{(1)} = -i2kz_n \frac{1 - \xi_n\cos\alpha}{\chi_n}. \tag{9a}$$

These are now substituted into the second matrix equation (1) to get the scattered mode amplitudes H_m, represented as the lower line and signs of (8) leading to a zero-order solution $H_0^{(0)} = 1$. To the first order in H_m we obtain

$$H_m^{(1)} = S_m^{(1)} = -i2kz_m \frac{1 - \xi_m\cos\alpha}{\chi_m}. \tag{9b}$$

This is the "classic" perturbation result for the scattering amplitudes dating to Rice [6]: nonspecular scatter is directly proportional to the surface height to first order. This "classic" Rice result also clearly demonstrates our point of contention: for vertical polarization at a perfectly conducting surface (Neumann boundary), the scattering amplitudes of (9b) remain constant as incidence angle approaches grazing ($\alpha \Rightarrow 0$). This is at odds with the more general result proven by Barrick [9], showing that the scattering amplitudes should decrease in direct proportion to α at grazing.

D. Propagation

When a plane wave is incident, the "propagated field" (or space wave) is normally taken to be the sum of the direct wave (incident field) and reflected wave, the latter for a planar interface being proportional to its Fresnel reflection coefficient. When the surface is rough, the specularly reflected field (often referred to as the "coherent" component of scatter for statistically rough surfaces) is defined as H_0. "Classic" perturbation theory above has found this to be $+1$ to lowest order, a result initially derived by Rice and discussed in the Introduction. For a flat Neumann boundary, the reflection coefficient is indeed $+1$ for all angles of incidence. For a rough boundary, however, this result implies failure of energy conservation at grazing, as discussed in the Introduction. The effective surface impedance is defined from the expression for the specular reflection coefficient as follows:

$$R_V = H_0 \equiv \frac{\sin\alpha - \mathbf{z}}{\sin\alpha + \mathbf{z}} \quad \text{leading to } \mathbf{z} = \sin\alpha \frac{1 - H_0}{1 + H_0}. \tag{10}$$

To the lowest (zero) order where $H_0^{(0)} = +1$, the impedance of this rough Neumann boundary is zero; let us, therefore, extend H_0 to the next nonzero order, which turns out to be second. Retain terms in (8b) through second order (with terms to zero order already removed) to obtain

$$ikz_1(1 - \xi_{-1}\cos\alpha)S_{-1}^{(1)} + S_0^{(2)}\sin\alpha$$
$$- (k\sin\alpha)^2 v_0 S_0^{(0)}\sin\alpha + ikz_{-1}(1 - \xi_1\cos\alpha)S_1^{(1)} = 0. \tag{11a}$$

For small α, we can ignore the third term involving $S_0^{(0)}$. Then, using (9a) in (11a) and solving for $S_0^{(2)}$, we get

$$S_0^{(2)} = -\frac{2k^2}{\sin\alpha}\sum_{n\neq 0}|z_n|^2 \frac{(1 - \xi_n\cos\alpha)^2}{\chi_n} \tag{11b}$$

where we have used the fact that $z_m z_{-m} = z_m z_m^* = |z_m|^2 = |z_{-m}|^2$ for $\zeta(x)$ real. Write the counterpart for H_0 using the lower signs

$$-ikz_1(1 - \xi_{-1}\cos\alpha)S_{-1}^{(1)} + S_0^{(2)}\sin\alpha$$
$$- ikz_{-1}(1 - \xi_1\cos\alpha)S_1^{(1)} = 2\sin\alpha H_0^{(2)}. \tag{11c}$$

Solving this for $H_0^{(2)}$ by employing (11c) and (9a) we obtain our result

$$H_0^{(2)} = -\frac{2k^2}{\sin\alpha} \sum_{n\neq0} |z_n|^2 \frac{(1-\xi_n\cos\alpha)^2}{\chi_n}. \qquad (11d)$$

We can now substitute $H_0^{(0)} + H_0^{(2)}$ into the second of (10) to obtain the surface impedance of the rough Neumann boundary

$$\mathbf{z} = k^2 \sum_{n\neq0} |z_n|^2 \frac{(1-\xi_n\cos\alpha)^2}{\chi_n}. \qquad (12)$$

This is the 1-D version of the result obtained by Wait [2], Barrick [3], and Feynberg [4].

E. Why These "Classic" Results Fail at Grazing

Both of the above "classic" perturbation results are clearly at odds with the general findings of [9]: 1) nonspecular scattered energy does not vanish as the angle of the incident plane wave approaches grazing as it should and 2) the energy in the specularly reflected ray (zero-mode, $H_0^{(0)} + H_0^{(2)}$) increases without limit, catastrophically failing energy conservation. The latter is evident by examination of this quantity

$$H_0 \cong H_0^{(0)} + H_0^{(2)} = 1 - \frac{2}{\alpha\mathbf{z}}$$
$$\Rightarrow -\frac{2}{\alpha\mathbf{z}} \Rightarrow -\infty \quad \text{as } \alpha \Rightarrow 0. \qquad (13)$$

This depiction of the interaction at grazing has the total energy in the "propagated" field (sum of incident and reflected plane waves) approaching infinity, even though the energy in the causative incident field is finite. In addition, the total energy in the "diffuse" (nonspecular) scattered modes $H_m^{(1)}$ remains constant in this limit. What went wrong with the above perturbational derivation (as well as that of Rice [6]) in the grazing limit?

This becomes clear by examining (8) above. The right-side vector, i.e., the "excitation" that drives the equation system represented by the upper sign/lines, contains only one element: $2\sin\alpha$ in (8b). This vanishes in the grazing limit. Except for the middle term in S_0, however, the left side of (8b) clearly remains finite. Thus, the entire system of equations for the surface currents defined by S_n has become indeterminate in the grazing limit. If one ignores this fact but later decides to set $\alpha \Rightarrow 0$ in the "classic" results for reflection and scatter, one cannot expect the results to remain valid when the system of equations that produced them had already broken down.

III. VALID PERTURBATION EXPRESSIONS BELOW THE BREWSTER ANGLE

A. Scatter

We overcome the failure of the "classic" perturbation (8) at grazing in the following way. Barrick [9] has proven that the surface currents/fields decrease in direct proportion to α, the incidence angle above grazing, for all rough surfaces. In addition, all of the scattering amplitudes except H_0 also decrease with α

near grazing. Hence, let us, therefore, expand these quantities in powers of α

$$S_n = s_n'\alpha + s_n''\alpha^2; \quad H_n = h_n'\alpha + h_n''\alpha^2 \quad \text{for } n \neq 0$$
$$H_0 = H_0^{(0)} + h_0'\alpha + h_0''\alpha^2. \qquad (14)$$

Substitute these into (8) and group terms in like powers of α. Also, recognize kz_n as a perturbational ordering parameter in the sizes of the terms of the equations. Doing so, one obtains the following equation sets:

$$\pm ikz_m(1-\xi_m)s_0' + \chi_m s_m' + \cdots + O(2)$$
$$= \begin{cases} 0 \\ 2\chi_1 h_m' \end{cases} \quad \text{for } m \neq 0 \qquad (15a)$$

$$\pm i \sum_{\substack{n=-N \\ n\neq0}}^{N} kz_{-n}(1-\xi_n)s_n' + O(3)$$
$$= 2\begin{cases} 1 \\ H_0^{(0)} \end{cases} \quad \text{for } m = 0. \qquad (15b)$$

In the same way, one obtains the following equations for terms multiplied by α^2

$$\pm ikz_m(1-\xi_m)s_0'' + \chi_m s_m'' + \cdots + O(2)$$
$$= \begin{cases} 0 \\ 2\chi_1 h_m'' \end{cases} \quad \text{for } m \neq 0 \qquad (16a)$$

$$s_0' \pm i \sum_{\substack{n=-N \\ n\neq0}}^{N} kz_{-n}(1-\xi_n)s_n'' + O(3)$$
$$= 2\begin{cases} 0 \\ h_0' \end{cases} \quad \text{for } m = 0. \qquad (16b)$$

Each of the upper sets of equations is solved to obtain the unknown surface current coefficients s_m' and s_m''. First, solve (15a) and (16a) for s_m' and s_m'' in terms of s_0' and s_0'' and substitute these into (15b) and (16b), respectively, to obtain

$$s_0' \sum_{\substack{n=-N \\ n\neq0}}^{N} \frac{|kz_n(1-\xi_n)|^2}{\chi_n} = 2 \qquad (17a)$$

$$s_0' + s_0'' \sum_{\substack{n=-N \\ n\neq0}}^{N} \frac{|kz_n(1-\xi_n)|^2}{\chi_n} = 0. \qquad (17b)$$

Thus, we end up with the following solutions for s_0' and s_0'', which we substitute into (16a) and (16b) to get subsequent solutions for s_m' and s_m''

$$s_0' = \frac{2}{\sum_{\substack{n=-N \\ (n\neq0)}}^{N} \frac{|kz_n(1-\xi_n)|^2}{\chi_n}} \qquad (18a)$$

$$s_0'' = \frac{2}{\sum_{\substack{n=-N \\ (n\neq0)}}^{N} \frac{|kz_n(1-\xi_n)|^2}{\chi_n}} \qquad (18b)$$

$$s_m' = \frac{-2ikz_m(1-\xi_m)}{\chi_m \sum_{\substack{n=-N \\ (n\neq0)}}^{N} \frac{|kz_n(1-\xi_n)|^2}{\chi_n}} \qquad (18c)$$

$$s_m'' = \frac{2ikz_m(1-\xi_m)}{\chi_m \sum_{\substack{n=-N \\ (n\neq0)}}^{N} \frac{|kz_n(1-\xi_n)|^2}{\chi_n}}. \qquad (18d)$$

When (17) and (18) are substituted back into the lower sets of (15) and (16) to solve for the scattered mode coefficients, we obtain the same identities between the first-order s_m and h_m as in the "classic" case treated earlier, i.e.,

$$h'_m = s'_m; \quad h''_m = s''_m$$
$$h'_0 = s'_0; \quad \text{but in this case, } H_0^{(0)} = -1. \tag{19}$$

Observe that the quantities s_m and h_m for $m \neq 0$ are smaller than s_0 and h_0 by one perturbation order in kz_n, as assumed earlier. However, we note what at first seems puzzling: (18) go to infinity as our "perturbation parameter" kz_n becomes sufficiently small. This seems unacceptable in a perturbation approach since we expect a stable result as the perturbation parameter vanishes. However, we have argued that these hold only in the limit of very small incidence angle α. Hence, this imposes a restriction on α under which the results of this section are valid; when α exceeds this limit, one must revert to the "classic" perturbation solutions of Section II. This "transition" region and the criterion for finding α_t that it imposes is found by setting $S_0 = s'_0 \alpha_t$ from this section (18a) equal to $S_0 = 2$ from the preceding "classic" perturbation solution to obtain

$$s'_0 \alpha_t = \frac{2\alpha_t}{\sum_{\substack{n=-N \\ (n \neq 0)}}^{N} \frac{|kz_n(1-\xi_n)|^2}{\chi_n}} \simeq 2$$

giving

$$\alpha_t = \sum_{\substack{n=-N \\ (n \neq 0)}}^{N} \frac{|kz_n(1-\xi_n)|^2}{\chi_n}. \tag{20}$$

As we shall see in the next section, the expression on the right turns out to be the effective impedance of this rough Neumann boundary, which is coincidentally identical to that found earlier in (12) using the "classic" perturbation approach.

B. Propagation

If we were to use the "classic" perturbation results of Section II (or those of Rice [6]) for the reflected field mode expanded for small α, we would obtain

$$H_0 \simeq H_0^{(0)} + H_0^{(2)} = 1 - \frac{2k^2}{\alpha} \sum_{n \neq 0} |z_n|^2 \frac{(1-\xi_n \cos\alpha)^2}{\chi_n}. \tag{21a}$$

Using the more exact, small-α results of this section for the same reflected field mode, we obtain

$$H_0 \simeq H_0^{(0)} + h'_0 \alpha = -1 + \frac{2\alpha}{k^2 \sum_{n \neq 0} |z_n|^2 \frac{(1-\xi_n \cos\alpha)^2}{\chi_n}}. \tag{21b}$$

When both of these are substituted into the defining equation for the surface impedance (10) near grazing, i.e., $\mathbf{z} = \alpha(1 - H_0)/(1 + H_0)$, it is quite surprising that both give identically the same result, i.e., [4, eq. (12)] derived more than 50 years ago by Feynberg . At grazing ($\alpha \Rightarrow 0$), this is

$$\mathbf{z} = k^2 \sum_{n \neq 0} |z_n|^2 \frac{(1-\xi_n)^2}{\chi_n}$$
$$\Rightarrow k^3 \int_{-\infty}^{+\infty} \frac{\mathbf{S}(k\eta)\eta^2 \, d\eta}{\sqrt{1-(1-\eta)^2}} \tag{22}$$

where the integral form converts the discrete Fourier coefficients z_n into a continuous 1-D average roughness height spectrum $\mathbf{S}(\kappa)$ at surface wavenumber κ; the normalized wavenumber is defined as $\eta \cong \kappa/k$. Thus, the general effective impedance (12), which includes incidence angle, is valid over a wide span all the way to grazing. As we shall see, this expression is slowly varying as grazing is approached, becoming constant in this limit.

Yet, of the two expressions for the reflected field (21a) and (21b), it is clear that the first, obtained by "classic" perturbation, goes to infinity as incidence angle approaches grazing and, hence, cannot correctly represent the interaction at shallow angles. Equation (21b) approaches $-1 + 2\alpha/\mathbf{z}$, which cancels the incident plane wave field so that the sum of the two then varies as α; in addition, all of the scattered field modes derived in this section given by (14) and (18) also vanish in direct proportion to α so that an energy balance between the propagating and scattered fields is obtained. Note that the reflected field at any flat but homogeneous interface between air and a lower medium also varies as $-1 + 2\alpha/\mathbf{z}$, as seen from (10), with the singular exception of the pure flat Neumann boundary, where it is always $+1$.

C. Example—Cosine Profile

The issues and interactions at play for the Neumann boundary near grazing can be further elucidated by studying a simple example: a cosine height profile $\zeta(x) = A\cos(\kappa x)$ that satisfies the perturbation requirements. Take the radio wavelength to be unity so $k = 2\pi$. Select $\kappa = 0.8$ k so the surface spatial period is 1.25, resulting in only two propagating modes for a near-grazing incidence regime. In particular, we study the region where $0° < \alpha < 10°$. Hence, the scatter angles of the two propagating modes remain sufficiently high over this region that Wood's anomalies are avoided for the incidence angle region between $0° < \alpha < 10°$, i.e., none of the propagating modes passes below the horizon, which would produce a discontinuity in energy apportionment at that angle.

To satisfy perturbation theory, let $A = 0.025$ so that $kA = 0.157$ and the maximum surface slope (the arctangent of κA) is 7.16°. To verify the perturbation approximations being discussed in this paper, we employ the full modal approach of Barrick [9]. It turns out that truncating this system to only three equations is adequate to obtain good accuracy for this simple example, which we verified by using a 7×7 system.

Both the exact modal result and the perturbation solution (12) above predict an effective surface impedance $z = 0.0040 - i0.0024$ for $0° < \alpha < 5°$. Above 5°, they change only in the second decimal, so that at 10°, they both become $\mathbf{z} = 0.0041 - i0.0026$. This demonstrates our claim that the effective impedance due to roughness approaches a constant at grazing like that for most flat interfaces over dense media.

Figs. 1 and 2 show how perturbation theory results exhibit the behavior claimed by Barrick [9], focusing here on the case where the incidence angle approaches grazing. In Fig. 1, we show the lowest two propagating modes H_1 and H_2 as well as the lowest evanescent mode H_{-1}. (Evanescent means the z-directed wavenumber, defined as $k_{\chi m}$, becomes pure imaginary rather than pure real, so that the field produced by this
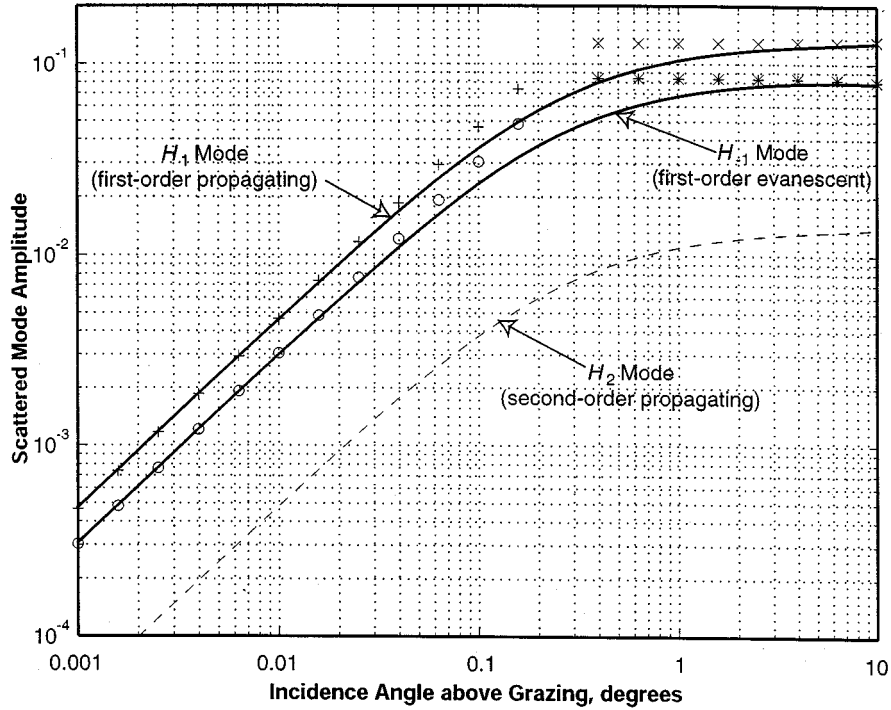
Fig. 1. Lowest order scattering amplitudes or modes. Curves are obtained from exact solutions for sinusoidal Neumann profile [9]. Points are first-order perturbation theory results; x,∗ are "classsic" perturbation theory predicting no grazing angle dependence, and +, o are grazing-limit perturbation theory derived herein.

mode attenuates exponentially with height above the surface.) The solid and dashed curves are obtained from inversion of the 7×7 exact modal matrix solution for the Neumann sinusoid [9]. One observes two distinct regions, with a transition near $0.3°$. Below this value, all of the scattered field mode amplitudes have a linear dependence on incidence angle α. Above this value, the scatter amplitudes tend to a constant. The overlying points are the results of perturbation theory: 1) the "x" and "∗" come from the "classic" perturbation theory reviewed in Section 2 and 2) the "+" and "o" come from the grazing-limit perturbation treatment derived in this section given in (18) and (19). On the log–log plot these points follow the predicted linear-α and constant dependences of the two different perturbational solutions we examined in Sections II and III, respectively. Since we derived explicit perturbational results here only to first order, no points accompany the dashed amplitude mode H_2, which is second order. The general linear-α behavior of these modes was established in [9]. Equation (14) here is our newly derived perturbation-limit expression that supports that general behavior.

Fig. 2 shows the specularly reflected plane wave mode H_0. Again, the solid and dashed curves come from the exact solution [10] applied to our Neumann sinusoid. The points result from the use of the perturbation-theory roughness-modified surface impedance of (12), which was shown to be valid above, through, and below the transition region in α. The points are not distinguishably different from the exact results. The interpretation of the transition region is clear from this plot: the "dip" in the amplitude is a Brewster-angle phenomenon exhibited by the Fresnel specular reflection coefficient at any planar interface above a more dense homogeneous lower medium for TM (vertical) polarization. The phase is changing from $0°$ above

this Brewster angle (about $0.3°$ for this profile) to $180°$ below it. This example demonstrates the claim in [9] that rough pure Neumann boundaries exhibit a Brewster-angle phenomenon at some angle. Also supported is the more general claim that the specularly reflected plane-wave mode at any rough boundary (Dirichlet, Neumann, or general impedance) must approach -1 at grazing, thereby canceling the incident plane wave.

IV. CONNECTION BETWEEN PROPAGATION AND SCATTER AT GRAZING INCIDENCE

The perturbation results below and above the Brewster-angle transition are explained by considering both propagation and scatter. Recall that we are dealing with a rough surface of infinite extent (rather than a patch or cell of roughness) and we are allowing only the incidence angle to vary near grazing.

A. Propagation Factor for Incidence Very Near Grazing

Equation (19) can be expressed in an interesting form that reveals the meaning of the interaction near grazing. Note that (19) for the low-angle scattered modes is merely (9b) for the high-angle modes divided by the effective surface impedance, i.e.,

$$h'_m \alpha = \frac{H_m^{(0)} \alpha}{\mathbf{z}} \qquad (23a)$$

as $\cos \alpha \Rightarrow 1$ in this small grazing-angle region. The "classic" first-order perturbation scatter result expressed as $H_m(0)$ in (9b) is independent of α in the low-grazing limit, i.e., it becomes constant; this was its failing near grazing.
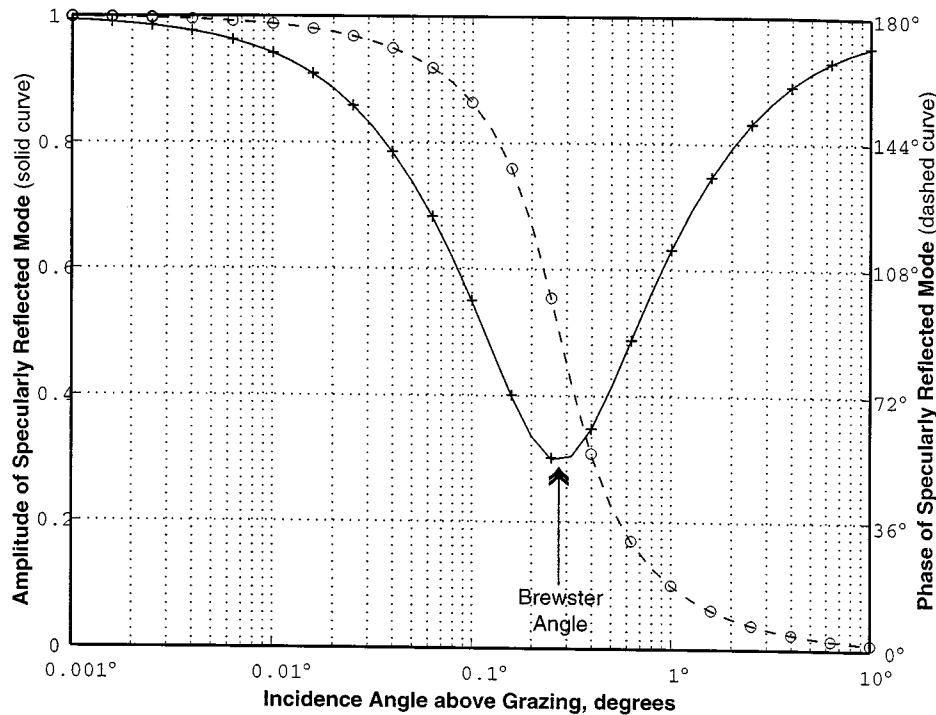
Fig. 2. Zero-order or specularly reflecting mode. Curves are obtained from exact solutions for sinusoidal Neumann profile [9]. Points are based on the roughness-modified surface impedance obtained from perturbation theory.

If one were to postulate a plane-wave illuminating a point at or near the surface, the total field would be the sum of the direct and reflected rays, tending to zero phase-path difference between rays exactly on the surface at grazing. Thus, one can write a "propagation factor" F to describe the sum of these two rays (assuming unity incident field strength) as

$$2F \equiv 1 + R_v(\alpha) = 1 + \frac{\sin\alpha - \mathbf{z}}{\sin\alpha + \mathbf{z}}$$
$$= \frac{2\sin\alpha}{\sin\alpha + \mathbf{z}} \Rightarrow \frac{2\alpha}{\mathbf{z}} \quad \text{as } \alpha \Rightarrow 0. \qquad (23\text{b})$$

Hence, (23a) takes on the following interpretation. The "classic" perturbation scatter result with constant-α behavior near grazing (when multiplied by the "propagation factor" F that includes the effect of the field reflected from the rough surface with effective impedance $\mathbf{z}$) is identically the solution for scatter below the Brewster angle. This means one can interpret the direct dependence of the scattered field on α near grazing from an infinite rough surface as due to propagation, i.e., the sum of the direct and specularly reflected fields producing the scatter must cancel in direct proportion to α near grazing for any imperfect planar boundary.

B. Plane-Wave Perturbation Scatter Theory Near Grazing Including Finite Surface Impedance/Admittance

Barrick derived expressions [9, appendix; eq. (24)] for bistatic scatter cross sections when a plane wave is incident on a slightly rough impedance/admittance boundary. Given in terms of the intrinsic surface material impedance $\mathbf{z}$ or admittance $\mathbf{y}$ for vertical or horizontal polarization, respectively, it has a form similar to the first equation of our Introduction—but modified by "propagation factors" that account for how the

energy gets to and from the scattering surface as discussed in the preceding section

$$\sigma^0_{vv,hh} = \pi k^3 S(k(\cos\alpha - \cos\beta)) \left| \frac{\sin\alpha}{\sin\alpha + \mathbf{z},\mathbf{y}} \right|^2$$
$$\times \left| 1 - \cos\alpha\cos\beta - \mathbf{z}^2, \mathbf{y}^2 \right|^2 \left| \frac{\sin\beta}{\sin\beta + \mathbf{z},\mathbf{y}} \right|^2. \quad (24)$$

Fuks *et al.* [15] derive this result rigorously for a slightly rough Neumann boundary, but where $\mathbf{z}$ now includes the effects of roughness, as in [15, eq. (53)].

Now, going to the limit of grazing incidence at backscatter for vertical polarization, one simplifies the bracketing "propagation factor" expressions (as done in the preceding section) to find

$$\sigma^0_{vv} \Rightarrow 4\pi k^3 S(2k) \left| \frac{\alpha}{\mathbf{z}} \right|^4 \qquad (25)$$

where it is assumed that $\mathbf{z}$ is small compared to unity. The effective impedance $\mathbf{z}$ of course, includes the effects of roughness calculated in (22) for the Neumann boundary.

C. Why Finite Sea Scatter Is Seen by HF/VHF Radars at Grazing

The results of the previous section thus lead to a resolution of the following quandary, "Why does one see a large, nonzero HF return from the sea with vertical polarization at grazing although exact theories predict zero backscatter?" A pulse-limited radar cell is not of infinite extent. One can analyze the return as seen above in terms of the interplay between propagation and scatter. First, propagate the energy from the radar to the cell being observed, defined by the effective pulse width and the azimuthal beamwidth. The energy at the cell depends on the "propagation factor" over the medium between the radar and the cell. If plane waves adequately describe the propagation, then the sum

of the direct and reflected rays is the propagation factor and this will cancel, exhibiting the behavior discussed in the previous section. Radiation from a dipole source (i.e., a simple antenna) near grazing, however, as originally derived by Sommerfeld [12] can be expressed in terms of a "Norton surface wave" [13]. At grazing, its unique propagation factor must replace the free-space factor derived above. This heuristic suggestion is discussed by Barrick in greater detail [9], [11] and was rigorously justified by the compensation theorem of Monteath [14] in [11]. Our purpose here is to elucidate the rationale rather than review the more rigorous justification.

At grazing above any mean planar interface, the Norton propagation factor for radiation from an antenna, replacing the plane wave propagation factor we called F in Section III, is unity from the near-field zone, out to a point called the "numerical distance," e.g., Wait [1]. The near-field distance, R, for a dipole is defined from $kR = 1$, while the numerical distance D is defined from $kD = |2/\mathbf{z}^2|$, where k is the radio wavenumber and $\mathbf{z}$ is the effective normalized impedance of our surface. Hence, for sea-type surfaces where $\mathbf{z}$ is small, the numerical distance can extend out tens of kilometers at low HF. Within this distance from the radar antenna, therefore, the total field reaching the radar cell is not zero as predicted by plane wave analysis, even though the incidence angle may be exactly grazing; the vertically polarized sea echo return is, therefore, finite and, in fact, generally strong. Beyond the numerical distance, the Norton attenuation factor asymptotically approaches $F = |\mathbf{z}^2/kr|$, which means one-way field strength decreases with distance from the source as $1/r^2$.

In reality, for the sea at HF, earth curvature and diffraction beyond the horizon are more relevant than the flat-plane formulas above; see Wait [1] or Barrick [3]. The close-in behavior is similar, however, with $F = 1$ out to ~20–30 km at 10 MHz over the sea. Beyond this point, the propagation factor is given in terms of a residue series obtained from an asymptotic evaluation of the Watson transform result for dipole radiation above a sphere [1].

Although we have focused on propagation from the radar to the cell, there is an analogous factor involved in scatter from the cell back to the receiver. If transmitter and receiver are colocated (a backscatter geometry), the two factors are identical and the radar equation for power contains the factor F^4; see [9] for further discussion.

V. GRAZING REGION AT A ROUGH DIRICHLET BOUNDARY

For comparison and completeness, we include analogous results for horizontal polarization at a slightly rough perfectly conducting 1-D surface: the Dirichlet boundary. The classic Rice results discussed in the Introduction do not have difficulties for this case since the reflection coefficient is well behaved near grazing, tending to -1. Just as with our definition of surface impedance from the vertical reflection coefficient (10), we define an effective normalized surface admittance $\mathbf{y}$ in terms of the horizontal reflection coefficient

$$R_H = \frac{\sin\alpha - \mathbf{y}}{\sin\alpha + \mathbf{y}}, \quad \text{which leads to}$$

$$\mathbf{y} = \sin\alpha \frac{1 - R_H}{1 + R_H}. \qquad (26)$$

Fitzgerald [16] invoked results of phase perturbation theory developed by Maradudin [17], [18] to work with the reflectivity for horizontal polarization for m a 1-D Dirichlet boundary as modified by slight roughness. We generalize Fitzgerald's [16, eq. (3)] for the reflectivity, which is the absolute square of our complex reflection coefficient (26), i.e., her $R(\theta_0)$ is our $|R_H|^2$

$$\ln R_H = i\pi - 2k\sin\alpha$$
$$\times \int_{-\infty}^{\infty} S(k\cos\alpha - \kappa)\sqrt{k^2 - \kappa^2}\, d\kappa \qquad (27)$$

where $k = \omega/c$ is the radio wavenumber defined in terms of the radian frequency ω and the speed of light c. Her integral, therefore, was the second term above, but multiplied by four instead of two and integrated over its real region, i.e., $-k < \kappa < k$.

Substituting (25) above into (24), one simplifies by noting that $R_H \Rightarrow -1$ for any perfectly conducting Dirichlet surface in the limit of vanishing roughness. This implies that $\mathbf{y}$ is very large. Because $\ln(1-\delta) \Rightarrow -\delta$ for small δ, one therefore obtains

$$\frac{1}{\mathbf{y}} = k\int_{-\infty}^{\infty} S(k\cos\alpha - \kappa)\sqrt{k^2 - \kappa^2}\, d\kappa$$
$$\Rightarrow k^3 \int_{-\infty}^{\infty} S(k\eta)\sqrt{1 - (1-\eta)^2}\, d\eta \qquad (28)$$

where the right side (taken in the grazing limit $\alpha \Rightarrow 0$) should be compared to the right side of (22) for surface impedance of a rough Neumann boundary. The counterpart here to the discrete Fourier series on the left of (22) is

$$\frac{1}{\mathbf{y}} = k^2 \sum_{n \neq 0}^{\infty} |z_n|^2 \chi_n. \qquad (29)$$

Note that in the absence of roughness, the above equations give $1/\mathbf{y} = 0$, or $\mathbf{y} = \infty$, which is the correct admittance for a flat Dirichlet (perfectly conducting) plane. We use the previous sinusoidal profile of Section III as an example and calculate the grazing-angle dependence of the roughness-caused admittance, obtaining $\mathbf{y} = 49.6370 - i75.8218$ at grazing ($\alpha = 0°$) and $\mathbf{y} = 50.5560 - i76.0498$ at $\alpha = 10°$. Thus, like the impedance, the admittance is nearly constant in the region near grazing, exhibiting very little dependence on α due to roughness. Because $\mathbf{y}$ is large in terms of unity, however, the corresponding reflection coefficient R_H from (24) changes very little from -1 in this region, and exhibits none of the "Brewster-angle" type behavior seen with the other polarization (Fig. 1). The latter, nonmonotonic behavior of the reflection coefficient is a consequence of an impedance—or admittance—being less than unity.

One can now contrast the behavior of backscatter vs. polarization at a highly conducting surface for plane wave incidence by examining (24). For slightly rough Dirichlet boundaries, $\mathbf{y}$ is sufficiently large so the center factor is replaced by $\mathbf{y}^4$, cancelling the $\mathbf{y}^{-4}$ dominance in the denominators of the surrounding factors. Thus the limiting dependence near grazing for horizontal polarization becomes

$$\sigma_{hh}^0 \Rightarrow \pi k^3 S(2k)\alpha^4 \qquad (30)$$

and the scatter polarization ratio is $(\sigma_{hh}^0/\sigma_{vv}^0) \Rightarrow (|\mathbf{z}|^4/4)$. This is valid only for plane wave incidence, i.e., where propagation to and from the scatter region does not follow surface-wave radiation laws from dipole sources, as discussed earlier.

VI. CONCLUSION

When a plane wave is incident on a rough Neumann boundary of infinite extent, the general treatment of Barrick [9] shows that the scattered power decreases as the square of both the scatter and incidence angles, as either of these angles approaches grazing. "Classic" perturbation theory does not predict this behavior. In this paper, we have reformulated a perturbation approach that obtains closed-form solutions for scatter exhibiting the proper grazing angle behavior. Closer inspection reveals that these solutions (to first order) are identically the "classic" solutions divided by the effective normalized impedance of the roughened boundary (12) or (22).

The physical interpretation of this inverse dependence on impedance is illuminating. The sum of the incident and the specularly reflected plane waves—the reflection coefficient for the latter being defined in terms of the effective surface impedance—reduces to $2\alpha/\mathbf{z}$ in the grazing limit for points on the surface. Hence, the appearance of $F = \alpha/\mathbf{z}$ (referred to as the propagation factor with respect to free-space) in our grazing perturbation result for scatter means that both the sum of the incident and reflected plane waves (the "space wave" component), as well as the scattered fields, must vanish as incidence angle $\alpha \Rightarrow 0$. This also supports the explanation for why vertically polarized sea echo from a finite-sized radar cell approaches a nonzero constant when we deal with radiation and reception from antennas (e.g., vertical dipoles) near the surface. One must interpret propagation to and from the surface scattering cell separately from scatter, and employ a factor F appropriate to dipole radiation, rather than assuming plane waves incident from infinity.

The transition between the two perturbation regions occurs at the pseudo Brewster angle for the rough Neumann boundary, i.e., the angle where the specular reflection has a minimum. This angle is equal to the arcsine of the real part of $\mathbf{z}$. Well above this angle, the "classic" perturbation results are valid, predicting nearly constant behavior with incidence angle. Below this angle, all scattered field amplitudes vanish in direct proportion to incidence angle α. It is noteworthy that both "classic" perturbation and our new grazing-limit perturbation solutions both give exactly the same result for the effective normalized surface impedance $\mathbf{z}$, as expressed in (12) and (22), which is also identical to that of Feynberg [4]. Hence, this perturbation result can be used everywhere: above, within, and below the transition zone. This effective impedance, due solely to the roughness, is well behaved, approaching a constant in the grazing limit. It exhibits none of the rapid Brewster-angle type variation in this region, as seen from our general equations and specific surface example. Hence, it is the natural link between scatter and propagation near grazing.

Horizontal polarization at a Dirichlet boundary introduces an admittance that is the counterpart of the impedance, decreasing from infinity at a smooth interface to a finite but large value when slight roughness is present. Both it and the specular reflection coefficient are nearly constant with angle near grazing. Classic perturbation methods and results for propagation and scatter, therefore, experience no difficulties in this case.

REFERENCES

[1] J. R. Wait, *Electromagnetic Waves in Stratified Media*.   New York: Pergamon, 1962.
[2] ——, "On the theory of radio propagation over a slightly roughened curved earth," in *Electromagnetic Probing in Geophysics*, J. R. Wait, Ed.   Boulder, CO: Golem, 1971, pp. 370–381.
[3] D. E. Barrick, "Theory of HF/VHF propagation across the rough sea," *Radio Sci.*, pt. I, II, vol. 6, pp. 517–533, 1971.
[4] E. Feynberg, "On the propagation of radio waves along an imperfect surface," *J. Phys.*, vol. 9, pp. 317–330, 1944.
[5] L. Rayleigh, *Theory of Sound*.   London, U.K.: Macmillan, 1929, vol. II, pp. 89–96.
[6] S. O. Rice, "Reflection of electromagnetic waves from slightly rough surfaces," in *Theory of Electromagnetic Waves*, M. Kline, Ed.   New York: Wiley, 1951, pp. 351–378.
[7] V. I. Tatarskii and M. Charnotskii, "Universal behavior of scattering amplitudes from a plane in an average rough surface for small grazing angles," *Waves Random Media*, vol. 8, pp. 29–40, 1998.
[8] ——, "On the universal behavior of scattering from a rough surface for small grazing angles," *IEEE Trans. Antennas Propagat.*, vol. 46, pp. 67–72, Jan. 1998.
[9] D. E. Barrick, "Grazing behavior of scatter and propagation above any rough surface," *IEEE Trans. Antennas Propagat.*, vol. 46, pp. 73–83, Jan. 1998.
[10] ——, "Near-grazing illumination and shadowing of rough surfaces," *Radio Sci.*, vol. 30, pp. 563–580, 1995.
[11] ——, "First-order theory and analysis of MF/HF/VHF scatter from the sea," *IEEE Trans. Antennas Propagat.*, vol. AP-20, pp. 2–10, Jan. 1972.
[12] A. N. Sommerfeld, "The propagation of waves in wireless telegraphy," *Ann. Phys.*, ser. 4, vol. 28, pp. 665–682, 1907.
[13] K. A. Norton, "Propagation of radio waves over a plane earth," *Nature*, vol. 135, pp. 954–955, 1935.
[14] G. D. Monteath, "Application of the compensation theorem to certain radiation and propagation problems," *Proc. Inst. Elect. Eng.*, pt. III, vol. 98, pp. 23–30, 1951.
[15] I. M. Fuks, V. I. Tatarskii, and D. E. Barrick, "Behavior of scattering from a rough surface at small grazing angles," *Waves Random Media*, vol. 9, pp. 295–305, 1999.
[16] R. Fitzgerald, "Reconstruction of the surface power spectrum from reflectivity data," *Opt. Lett.*, vol. 24, pp. 364–366, 1999.
[17] J. Shen and A. Maradudin, "Multiple scattering of waves from random rough surfaces," *Phys. Rev. B*, vol. 22, pp. 4234–4240, 1980.
[18] J. Sanchez-Gil, A. Maradudin, and E. Mendez, "Limits of validity of three perturbation theories of the specular scattering of light from one-dimensional, randomly rough, dielectric surfaces," *J. Opt. Soc. Amer. A*, vol. 12, pp. 1547–1558, 1995.

Donald E. Barrick was born is Tiffin, OH. He received the B.E.E., M.Sc., and Ph.D. degrees in electrical engineering from The Ohio State University, Columbus.

   He taught radar and electromagnetics at The Ohio State University. He has served as a Fellow at Battelle Memorial Institute, organized the Sea State Studies Division at NOAA's Wave Propagation Laboratory (an ocean remote sensing group), and led industry groups in electromagnetics and radar cross section design/control. In the mid 1980s, he founded and now serves as President of CODAR Ocean Sensors, Ltd., Los Altos, CA, where he has been involved in creating and developing the SeaSonde line of products, high-frequency compact coastal radars that map ocean surface currents in real time based on scatter from sea waves. His scientific interests include radar remote sensing, electromagnetics, rough surface scatter, antennas, and signal processing.

Rosa Fitzgerald was born in Lima, Peru, and became a U.S. citizen in 1985. She received the Ph.D. degree in physics from the University of California, Riverside.

   She was involved in two postdoctoral experiences involving electromagnetic scattering from surfaces and environmental physics. Currently, she is an Assistant Professor of physics at the University of Texas, El Paso. Her main research activities focus on electromagnetic scattering and its applications toward the environment.